

PALS Laser Interactions with Foam Targets

J. Limpouch^{1,5}, N. N. Demchenko², S. Yu. Gus'kov², A.I. Gromov², M. Kalal¹,
A. Kaspercuk³, V. N. Kondrashov⁴, E. Krousky⁵, K. Masek⁵, P. Pisarczyk⁶, T. Pisarczyk³,
V. B. Rozanov²

¹ Czech Technical University, FNSPE, Brehova 7, 115 19 Prague 1, Czech Republic

² P.N. Lebedev Physical Institute of RAS, Leninskyi Ave., 53, 117 924 Moscow, Russia

³ Institute of Plasma Physics and Laser Microfusion, 23 Hery St., 00-908 Warsaw, Poland

⁴ Troitsk Institute of Innovation and Thermonuclear Research, 142 190 Troitsk, Russia

⁵ Institute of Physics, AS CR, Na Slovance 2, 182 21 Prague 8, Czech Republic

⁶ Warsaw University of Technology, ICS, 15 Nowowiejska St., Warsaw, Poland

1. Introduction

Low density foam layers may be used for smoothing of laser imprint by thermal conductivity [1,2] or for suppressing of Rayleigh-Taylor instability [3]. They are also used in experiments [4] studying equation-of-state (EOS), and in astrophysics dedicated experiments [5].

The main goal of our work is to study energy transport through the low-density porous matter and to demonstrate a sufficient efficiency of thin foil acceleration together with substantial smoothing effect of the low-density foam absorber. The distinctive feature of these experiments succeeding to our previous work [6] is the laser pulse duration shorter than the time needed for full homogenization of the foam containing relatively large pores.

2. Experimental setup

PALS iodine laser facility [7] provided 400 ps (FWHM) pulse with the energy up to 600 J at the basic harmonic ($\lambda_1 = 1.32 \mu\text{m}$). The laser spot radius of normally incident beam on target placed out of the best focus was $R_L \approx 150 \mu\text{m}$. Laser irradiances were varied from $I \approx 10^{14} \text{ W/cm}^2$ up to $I \approx 10^{15} \text{ W/cm}^2$. No method of optical smoothing was used.

Most experiments were done with thick polystyrene foams of density 8–10 mg/cm³ and of typical pore diameter $D_p \approx 50\text{--}70 \mu\text{m}$. Other polystyrene foams and polyvinylalcohol (PVA) foam of density $\rho \approx 5 \text{ mg/cm}^3$, and of pore diameter $D_p \approx 5 \mu\text{m}$ were used. A 2 μm or 0.8 μm -thick aluminum foil was placed at the foam rear side in the majority of targets.

Plasma emission in x-ray region (photon energy $> 1.7 \text{ keV}$) was observed by the KENTECH low magnification x-ray streak camera placed in a side view. The temporal resolution was either 30 or 70 ps and spatial resolution of 50 μm was in the direction normal to the target surface (target depth). Optical diagnostics was carried out by means of 3-frame interferometric system with automated image processing technique [8].

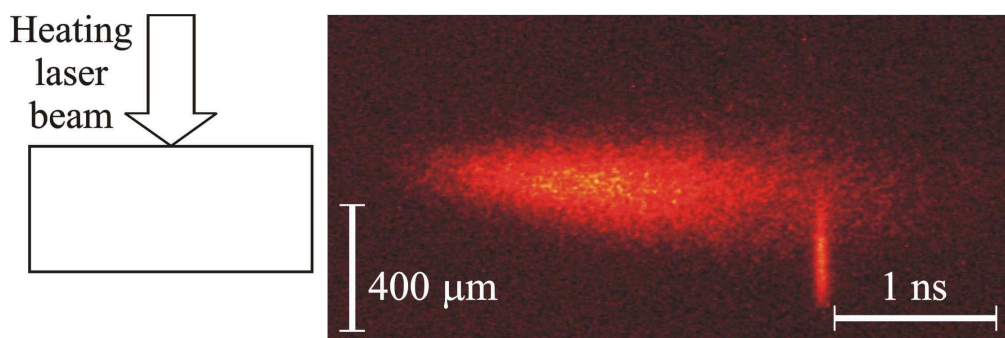


Fig. 1 X-ray streak record of interaction of 400 ps iodine laser ($\lambda=1.32 \mu\text{m}$) pulse of energy 92 J and beam radius $150 \mu\text{m}$ with $400 \mu\text{m}$ thick polystyrene foam of density $\rho \approx 9 \text{ mg/cm}^3$ and pore diameter $D_p \approx 50 - 70 \mu\text{m}$, $2 \mu\text{m}$ -thick Al foil is placed at the target rear side.

3. Experimental results

Very weak images at the X-ray streak camera sensitivity limit were recorded for the foam targets. Typical record taken from lateral view is presented in Fig. 1. The laser penetration depth may be estimated by the $50 \mu\text{m}$ -thickness of the immediately heated layer. Later, heat wave propagates into the foam material with velocity of approximately $\sim 6 \times 10^6 \text{ cm/s}$. Though the x-ray signal lasts for about 2 ns, the x-ray emitting zone covers only about one half of the foam thickness and no emission near the Al foil at the target rear side is detected. Consequently, the foil at the target rear side is supposed to be accelerated as a whole without significant expansion and its velocity can be measured by optical probing.

Experimental sequences of 3 interferometric pictures taken in one laser shot are presented in Fig. 2. While the rear side boundary of $400 \mu\text{m}$ thick polystyrene target with $2 \mu\text{m}$ Al foil on the rear side is sharp with no signs of low-density plasma behind the target, Al foil at the rear side of $100 \mu\text{m}$ PVA foam is heated and its expansion is later observed.

The position of the point P (rear side opposite to the laser beam centre) is measured with the precision of $5 - 10 \mu\text{m}$. The speed of the accelerated Al foil can be determined from the difference in point P positions in different frames. The speed of accelerated foil grows with the laser energy. Foil acceleration during the laser pulse is inferred for $100 \mu\text{m}$ thick PVA foam. For $400 \mu\text{m}$ thick polystyrene foams, the shock wave reaches the foil only 2-4 ns after the laser pulse, and the delay decreases with laser energy.

4. Computational simulations and analytical model

Simulations were performed in cylindrical geometry by two-dimensional Lagrangian hydrodynamics code ATLANT-HE including advanced treatment of laser propagation and

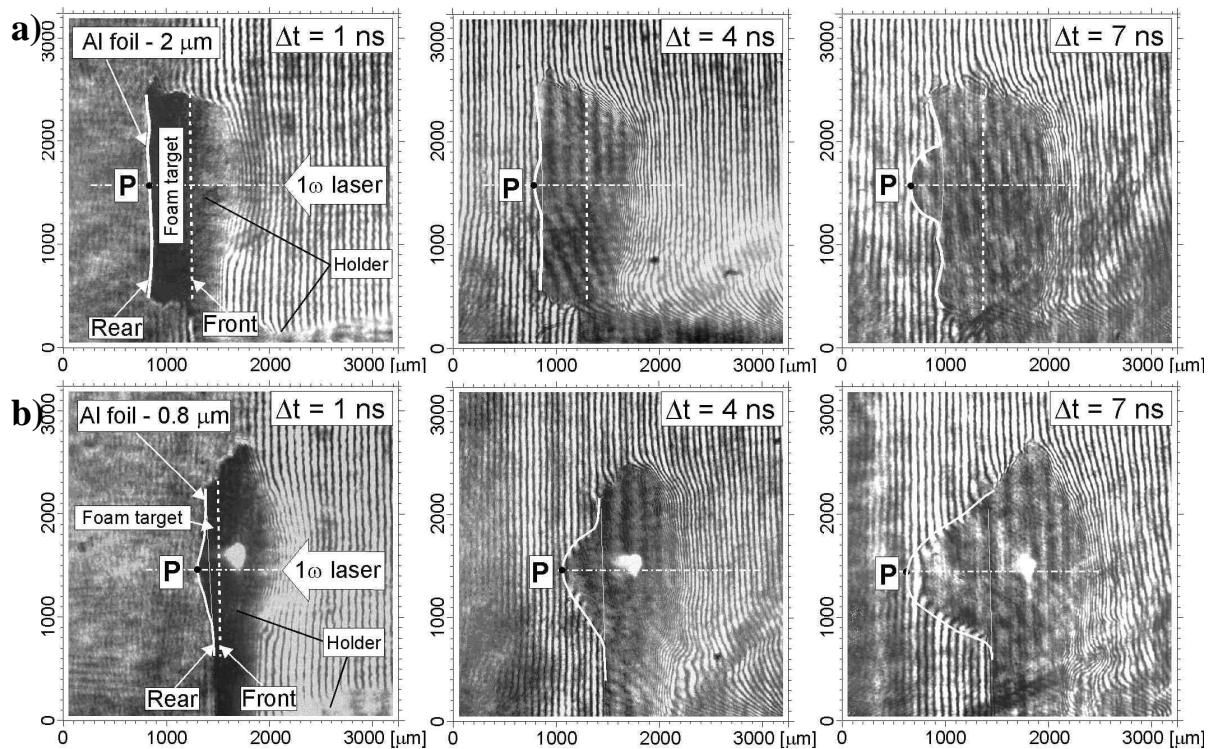


Fig. 2 Sequence of 3 interferograms recorded in one shot in time instants 1, 4 and 7 ns after the main 400 ps FWHM laser pulse maximum. Laser wavelength 1.32 μm and beam radius 150 μm on the targets. Parasitic effects of the target holder are denoted in the left pictures. a) Polystyrene foam of $\rho \sim 9 \text{ mg/cm}^3$, $D_p \sim 50 - 70 \mu\text{m}$, 400 μm thick and 2 μm thick Al foil at its rear side. Laser energy 173 J. b) PVA foam of $\rho \sim 5 \text{ mg/cm}^3$, $D_p \sim 5 \mu\text{m}$, 100 μm thick and 0.8 μm thick Al foil at its rear side. Laser energy 238 J.

absorption [9]. The code does not take into account fine scale structure of the foam and thus the time of the hydrothermal wave transit through the foam may be underestimated.

The calculated laser absorption was approximately 50%. Plasma radius essentially exceeds the laser beam radius on the target due to fast lateral heat transport in the low-density porous matter. A smooth shape of the accelerated foil is observed with the width considerably larger than the laser beam diameter. The fast electrons do not preheat unevaporated Al layer in simulations for the laser intensities $\leq 10^{15} \text{ W/cm}^2$ significantly.

Analytical model is based on assumption of spherical hydrothermal wave [10] propagating from laser absorption point. Time instants when the hydrothermal wave reaches the target rear side are in a good agreement with numerical simulations. However, the experimental data are by about 2 ns greater for 400 μm thick polystyrene foam. According to our opinion, such a fact is caused by the direct influence of the initial structure of foam on the target dynamics. The pressure accelerating the Al foil is calculated and the derived hydrodynamic efficiency is $\eta \approx 0.12$.

Laser energy	Target	v_{exp} (cm/s)	v_{simul} (cm/s)	V_{max} (cm/s)
92 J	(CH) _n	6.0×10^6	4.9×10^6	4.8×10^6
173 J	(CH) _n	8.0×10^6	8.2×10^6	6.7×10^6
238 J	(CH) _n	-----	1.1×10^7	8.2×10^6
238 J	PVA	1.4×10^7	3.5×10^7	1.32×10^7

Table 1 (CH)_n is 400 μm thick polystyrene foam with 2 μm Al foil and PVA is 100 μm thick PVA foam of density 5 mg/cm³ with 0.8 μm Al foil. Experimental and simulation velocities are represented by average values in the interval 4–7 ns after the laser maximum.

The foil velocities measured in the experiment, calculated in our simulations and via analytical model are compared in Table 1. The Al foil in PVA foam target is heated up to 800 eV in the simulation and its expansion leads to high velocity of the rear boundary.

5. Conclusions

Interactions of laser beam of iodine laser “PALS” with low-density foam targets have been investigated, both experimentally and theoretically. The speed of the heat wave inside polystyrene foam has been estimated $\sim 6 \times 10^6$ cm/s from the X-ray streak measurements. Hydrodynamic efficiency up to 12-14 % was calculated from the experimental data.

The experimental results are in a good agreement with our two-dimensional hydrodynamic calculations and with analytical model. The delay in the heat wave propagation in the foam in our experiments in comparison with our theoretical calculations is explained here by the phenomenon of non-equilibrium foam homogenization.

Partial support by grant INTAS-01-0572, and by IAEA project No. IFE-CRP, CZR-11655 is gratefully acknowledged. Czech authors were partly supported by Ministry of Education, Youth and Sports project LN00A100. Polish participants were supported in part by the EC contract HPRI-CT-1999-0053.

References

- [1] Desselberger M, Jones M W, Edwards J *et al.*, *Phys. Rev. Lett.* **68**, 1539 (1992).
- [2] Gus'kov S Yu, Zmitrenko N V, Rozanov V B, *JETP* **81**, 296 (1995).
- [3] Metzler N, Velikovich A L *et al.*, *Phys. Plasmas* **9**, 5050 (2002).
- [4] Batani D, Balducci A, Nazarov W *et al.*, *Phys. Rev. E* **63**, 046410 (2001).
- [5] Remington B A, Kane J, Drake R P *et al.*, *Phys. Plasmas* **4**, 1994 (1997)/
- [6] Kalal M, Limpouch J *et al.*, *Fusion Science & Technology* **43**, 275 (2003).
- [7] Jungwirth K, Cejnarova A, Juha L *et al.*, *Phys. Plasmas* **8**, 2495 (2001).
- [8] Pisarczyk T, Arendzikowski R *et al.*, *Laser & Particle Beams* **12**, 549 (1994).
- [9] Iskakov A B, Demchenko N N, Lebo I G *et al.*, *Proc. SPIE* **5228**, 143 (2003).
- [10] Gus'kov S Yu, Gromov A I *et al.*, *Laser & Particle Beams* **18**, 1 (2000).